

Stripe domains in multilayered magnetic media

V. O. Vas'kovskii, Yu. V. Ivanov, and G. S. Kandaurova

Ural State University

(Submitted April 16, 1976)

Zh. Eksp. Teor. Fiz. 71, 1905-1911 (November 1976)

A model of layered (stripe) domains is considered for a plate of a uniaxial ferromagnetic material with two thin magnetically hard surface layers. It is assumed that the plane walls of the original domains extend through the crystal and are pinned at the surface layers. The following theoretically predicted effects are detected experimentally: the appearance of stripe domains inside the original ones, and a discontinuous increase of the width of the original domains. The quantitative results of the calculation agree well with experimental data obtained from observations of the domain structure of orthoferrite crystals at various temperatures.

PACS numbers: 75.60.Fk

Investigation of the domain structure (DS) of magnetically inhomogeneous media is revealing new types of DS and new rules for their behavior, and is thereby broadening the possibilities for practical use of DS. Such media include metallic multilayer magnetically uniaxial films,^[1] monocrystalline iron garnet films with composition varying in layers,^[2,3] films with exchange anisotropy,^[4,5] thin orthoferrite plates with a deformed surface layer,^[6] and orthoferrite and iron garnet plates (films) with metallic layers deposited on their surface.^[7]

Among these inhomogeneous systems, a special place is occupied by plates with a magnetically hard surface layer. The domain configurations in this layer may possess great stability. For example, to change the so-called "shadow" DS in orthoferrite plates^[6] requires fields that exceed by several orders of magnitude the field intensities at which magnetization reversal of the low-coercivity part of the crystal occurs. The presence of a stable structure in the surface layer significantly influences the DS of the whole specimen.

In the simplest case, when the surface layer is uniformly magnetized, domains with magnetization antiparallel to the magnetization in the surface layer are separated from it by end-on domain walls (Fig. 1a). The possibility of formation of such end-on boundaries was demonstrated earlier.^[7-9] The effect of these additional walls on the DS of the crystal is equivalent to the action of a certain effective magnetic field $H_{\text{eff}} = \gamma_1 / M_s L$,^[7-9] where γ_1 is the surface energy density of the end-on domain walls, M_s is the saturation magnetization of the main part of the crystal, and L is the thickness of the plate (it is assumed that the thickness of the surface layer is negligibly small in comparison with L). In this situation the widths of adjacent stripe domains are different, even in the absence of an external magnetic field,^[9] and can be calculated by known methods.^[10] For this purpose it is sufficient to use instead of the external field H the sum $H + H_{\text{eff}}$.

More interesting is the case in which the surface layer is magnetized nonuniformly, i. e., has its own DS. One of the variants of this state, corresponding to the simplest layered structure, is shown schematically in Fig. 1b. The domain structure of the crystal is built under the surface structure, thereby preventing the formation

of end-on domain walls. But with change of the external conditions, for example of the temperature T , when the material constants change appreciably and yet the boundaries of the main domains remain pinned by the surface DS, it can be expected that the conformity of the surface and internal structures will be disturbed. What proves energetically advantageous is either the appearance, inside the original strip domains of width D , of new (secondary), thinner domains of width $d < D$ (Fig. 1c), or a discrete increase of the period of the internal DS (for example, threefold, as in Fig. 1d). The first effect is possible when the characteristic length $l = \gamma / 4M_s^2$ (γ is the surface energy density of ordinary domain walls) decreases, and accordingly the equilibrium width of the domains must decrease; the second, when l increases.

The relation between the parameters of the DS shown in Fig. 1c can be found from the following theoretical model. We shall suppose that the dimension D is fixed and is completely determined by the width of the domains in the magnetically hard surface layer, and that the magnetization in the domains is constant and oriented parallel to the axis of easy magnetization. The equilibrium value of d can be found by minimizing the sum of the magnetostatic and boundary energies. Here it is convenient to measure the total energy of the two-dimensional configuration shown in Fig. 1c from the energy of the basic DS (Fig. 1b) and to refer it to unit length of a stripe domain and to a half period of the magnetization distribution being considered. Thus the total energy E can be written in the form

$$E = E_m + 2L\gamma + 2d\gamma_1, \quad (1)$$

where E_m is the magnetostatic energy of the internal

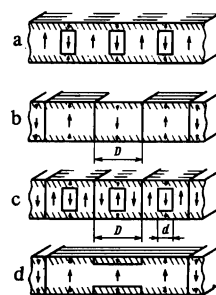


FIG. 1. Schematic representation of domain configurations realized in a crystal plate with magnetically hard surface layers.

(secondary) domains; it includes the magnetostatic self-energy of these domains and also their energy of interaction with the surface charges of the basic structure. E_m can be easily calculated by the method of the scalar potential, by solution of Laplace's equation with appropriate boundary conditions^[10]:

$$E_m = \frac{64}{\pi^2} M_s^2 D^2 \Xi_1 \left(\frac{d}{D}; \frac{L}{D} \right), \quad (2)$$

$$\Xi_1 = \sum_{n=0}^{\infty} (2n+1)^{-2} \sin \frac{\pi(2n+1)d}{2D} \left[\sin \frac{\pi(2n+1)d}{2D} - (-1)^n \right] \left[1 - \exp \left(-\frac{\pi(2n+1)L}{D} \right) \right]. \quad (3)$$

The condition for a minimum of the energy of the system, which determines the equilibrium domain configuration, has the form

$$\frac{\gamma_L}{M_s^2 D} = -\frac{16}{\pi} \Xi_2 \left(\frac{d}{D}; \frac{L}{D} \right), \quad (4)$$

$$\Xi_2 = \sum_{n=0}^{\infty} (2n+1)^{-2} \cos \frac{\pi(2n+1)d}{2D} \left[2 \sin \frac{\pi(2n+1)d}{2D} - (-1)^n \right] \left[1 - \exp \left(-\frac{\pi(2n+1)L}{D} \right) \right]. \quad (5)$$

Figure 2 shows, in reduced units, the variation of the width d/D of the internal domains, satisfying (4), with the energy $\gamma_L/M_s^2 D$ of the end-on domain walls, for several fixed values of the crystal thickness L/D . It is seen that with increase of the parameter $\gamma_L/M_s^2 D$ the equilibrium width of an internal domain decreases monotonically. But d/D never vanishes and never exceeds the value 0.4.

From analysis of (1) it also follows that the structure shown in Fig. 1c is stable for arbitrary d/D . But at the same time, significant decrease of d/D must lead to an unwarranted increase of the relative role of the boundary energy; then the configuration shown in Fig. 1c proves only metastable, while the structure shown in Fig. 1b becomes stable. The critical value of the parameter $\gamma_L/M_s^2 D$ at which nucleation (annihilation) of secondary domains occurs can be found from the condition $E=0$. If we set $\gamma_L(T) = \gamma(T)$, then this condition takes the form

$$\frac{2}{\pi} \Xi_1 \left(\frac{d}{D}; \frac{L}{D} \right) - \left(\frac{d}{D} + \frac{L}{D} \right) \Xi_2 \left(\frac{d}{D}; \frac{L}{D} \right) = 0. \quad (6)$$

By simultaneous numerical solution of equations (4) and (6), it was possible to construct a diagram (Fig. 3, curve 1) that determines the critical value of the param-

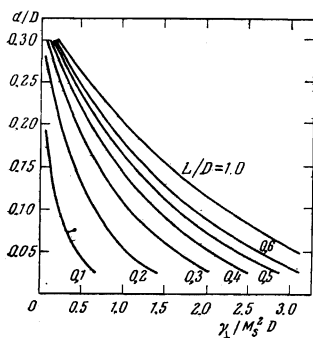


FIG. 2. Variation of reduced width d/D of secondary stripe domains with the parameter $\gamma_L/M_s^2 D$, for various values of L/D .

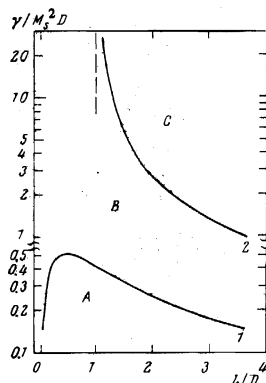


FIG. 3. Variation of the critical value of the parameter $\gamma/M_s^2 D$ with reduced plate thickness. In regions A, B, C the structures occur that are shown schematically in Figs. 1c, 1b, 1d respectively.

eter $\gamma/M_s^2 D$. In region A, the DS shown in Fig. 1c proves energetically more advantageous; in region B, the DS in Fig. 1b.

With increase of the parameter $\gamma/M_s^2 D$, the growth of the relative role of the boundary energy leads, in a perfect crystal, to increase of the width of the stripe domains. In our case, the period of the internal DS may not be arbitrary. It may be expected to change discretely, remaining a multiple of the period of the shadow DS in the surface layer. Then by equating the surface density of the total energy of the basic DS (Fig. 1b) to the surface density of the total energy of the DS with tripled period (Fig. 1d) and again assuming $\gamma = \gamma_L$, one can determine the boundary (Fig. 3, curve 2) between the regions B and C in which the structures described in Figs. 1b and 1d, respectively, are energetically more advantageous. In similar fashion one can show that the transition under consideration is preferred in comparison with a transition to a DS with doubled period.

The relations described are obviously only the initial stages of change of the basic structure (Fig. 1b) with decrease or increase of the parameter $\gamma/M_s^2 D$. After them one must expect transitions to structures with two, three, etc. secondary domains in a single basic one, and also transitions involving n -fold ($n > 3$) increase of the period of the internal DS.

We have investigated experimentally the DS of crystal plates of TmFeO_3 , DyFeO_3 , YFeO_3 , and $\text{Sm}_{0.55}\text{Tb}_{0.45}\text{FeO}_3$ with basal orientation, with a magnetically hard surface layer. In orthoferrites, a magnetically hard layer is formed in the process of mechanical polishing of the plates.^[6] In specimens of thickness $\sim 100 \mu\text{m}$ prepared in this manner, the DS realized at room temperature is similar to the structure described in Fig. 1b. This enables us to test the theoretical conclusions by experiment.

Figure 4 shows the equilibrium (after magnetic "shaking") DS of a TmFeO_3 crystal in the temperature interval 300–77 K. The DS was exhibited by means of the Faraday effect. The photographs in Figs. 4a–4e reflect the structure in a mechanically polished specimen, those in Figs. 4f–4i the structure in the same specimen subjected to annealing, i. e., without the magnetically hard surface layer. The temperature variation of the saturation magnetization and of the boundary energy density in TmFeO_3 is such that with lowering of the temperature

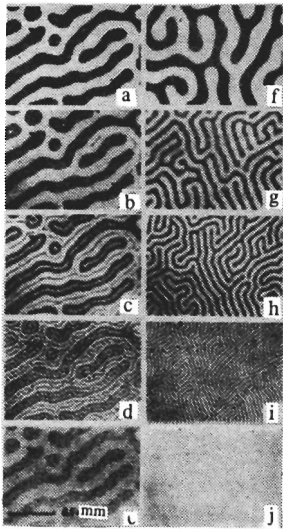


FIG. 4. Domain structure of $TmFeO_3$ at temperatures: a and f, 293 K; b and g, 155 K; c and h, 130 K; d and i, 100 K; e and j, 88 K. The specimen is in the state that results after mechanical polishing for a—e and after high-temperature annealing for f—i.

the width of the stripe domains decreases (Fig. 4f–4i). Furthermore, at $T \approx 90$ K there occurs in $TmFeO_3$ a reorientation of the axis of easy magnetization that is accompanied by disappearance of the contrast in the DS picture (Fig. 4j).

The behavior is different for the DS of a crystal with a magnetically hard surface layer, in which the DS corresponding to room temperature is fixed. Down to 170 K its form remains unchanged: the structure of the internal part of the plate exactly copies the shadow DS. Thus large temperature hysteresis is observed in the change of width of the domains, as compared with a perfect crystal. At lower temperature, in accordance with theoretical prediction, within the basic domains there appear minute domains of reverse magnetization (Fig. 4b), which within a small temperature interval grow into narrow secondary stripe domains (Fig. 4c). Further lowering of temperature causes them to bend and branch, and as a result there appear in each basic domain two or even three parallel internal domains (Fig. 4d). The width of these secondary internal domains changes inappreciably during the process of lowering the temperature.

We remark that at $T \approx 90$ K the contrast between domains diminishes abruptly; the DS in the volume of the crystal disappears (Fig. 4e). But in the surface layer there remains the shadow DS, corresponding completely to the DS that existed at room temperature (compare Figs. 4e and 4a). From this we can conclude that reorientation of the axis of easy magnetization does not occur in the deformed surface layer. A more striking delay of the reorientation of the easy axis can be observed in $Sm_{0.55}Tb_{0.45}FeO_3$ crystals. In them the DS of the main part of the crystal ceases to be exhibited at 240 K, whereas the surface shadow structure is retained down to 77 K.

Realization of the second theoretically indicated possibility, i. e., transition from the basic DS (Fig. 1b) to a structure in which each internal domain is arranged under three surface domains (Fig. 1d), was observed in

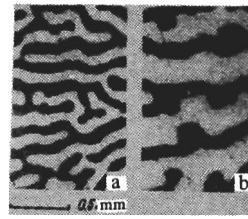


FIG. 5. Domain structure of $Sm_{0.55}Tb_{0.45}FeO_3$ at temperatures: a, 290 K; b, 590 K.

a mechanically polished crystal of $Sm_{0.55}Tb_{0.45}FeO_3$ when it was heated. The domain structure of this crystal is shown in Fig. 5. Enlargement of the domains begins at temperature 560 K, and at 590 K (Fig. 5b) a domain structure appears that is similar to the structure shown schematically in Fig. 1d.

It must be noted that with rise of temperature there is a sharp increase of the absorption of light by orthoferrite crystals, and direct observation of their DS becomes impossible at $T > 550$ K. Therefore the photographs of DS in Fig. 5b were obtained after the following operations. The specimen was heated to the necessary temperature, subjected to magnetic shaking, and then cooled to 520 K, where the record was made. It may be assumed that the DS characteristic of $T > 520$ K is retained because of the large temperature hysteresis, whose presence is corroborated by direct observations of the DS at lower temperatures.

The critical values of the parameter $\gamma/M_s^2 D$ determine the critical values of temperature T_1 and T_2 at which occur, respectively, nucleation of secondary stripe domains and abrupt increase of the width of the domains of the initial DS. Table I gives experimentally measured values $T_{1,2}(\text{exp})$ and calculated values $T_{1,2}(\text{theor})$ of the critical temperatures for specimens of $TmFeO_3$, $DyFeO_3$, and $Sm_{0.55}Tb_{0.45}FeO_3$. The values of $T_{1,2}(\text{theor})$ was estimated from the diagram in Fig. 3 by use of concrete values of L/D and of the variation of γ/M_s^2 with T as determined by us. It is seen that the agreement of the theoretical and experimental results is good. In the orthoferrite $Sm_{0.55}Tb_{0.45}FeO_3$ the reorientation of the axis of easy magnetization occurs before the temperature T_1 is reached.

On the other hand, in crystals of $DyFeO_3$ and $TmFeO_3$, in accordance with the diagram in Fig. 3, there is no transition to a structure with enlarged internal domains, since in these materials the ratio L/D is always less than unity. In yttrium orthoferrite, the saturation magnetization and the boundary energy density vary little with temperature; therefore over a broad temperature range no changes of the initial DS are observed.

In conclusion it should be remarked that the relation-

TABLE I. Experimental and theoretical values of the temperatures at which secondary domains appear (T_1) or the period of the basic DS increases threefold (T_2).

	L, μ	$D, \mu m$	$T_1(\text{exp}), K$	$T_1(\text{theor}), K$	$T_2(\text{exp}), K$	$T_2(\text{theor}), K$
$TmFeO_3$	48	112	140	140	—	—
$DyFeO_3$	88	152	175	160	—	—
$Sm_{0.55}Tb_{0.45}FeO_3$	113	70	—	—	560	590

ships observed may be valid to some degree in other multilayer systems also, if the DS in a magnetically hard layer (or layers) is sufficiently stable and does not change the change of the external conditions.

The authors thank V. K. Raev, A. M. Balbashov, and A. Ya. Chervonenkis for the orthoferrite crystals provided for the investigation.

¹A. Yelon, Phys. Thin Films 6, 205 (1971).

²Y. S. Lin, P. J. Grundy, and E. A. Giess, Appl. Phys. Lett. 23, 485 (1973).

³H. Uchishiba, H. Tominaga, T. Obokata, and T. Namikata,

IEEE Trans. Magn. MAG-10, 480 (1974).

⁴A. A. Glazer, R. I. Tagirov, A. P. Potapov, and Ya. S. Shur, Fiz. Met. Metalloved. 26, 289 (1968) [Phys. Met. Metallogr. 26, No. 2., 103 (1968)].

⁵Yu. G. Sanoyan and K. A. Egiyan, Fiz. Met. Metalloved. 38, 231 (1974) [Phys. Met. Metallogr. 38, No. 2, 1 (1974)].

⁶A. V. Antonov, A. M. Balbashov, and A. Ya. Chervonenkis, Izv. Vuzov Ser. Fiz., No. 5, 146 (1972).

⁷T. W. Liu, A. H. Bobeck, E. A. Nesbitt, R. C. Sherwood, and D. D. Bacon, J. Appl. Phys. 42, 1360 (1971).

⁸P. P. Luff and J. M. Lucas, J. Appl. Phys. 42, 5173 (1971).

⁹J. M. Lucas and P. P. Luff, AIP Conf. Proc. 5, Part 1, 145 (1972).

¹⁰C. Kooy and U. Enz, Philips Res. Rep. 15, 7 (1960).

Translated by W. F. Brown, Jr.

Electron density distribution for localized states in a one-dimensional disordered system

A. A. Gogolin

L. D. Landau Institute of Theoretical Physics, USSR Academy of Sciences

(Submitted April 20, 1976)

Zh. Eksp. Teor. Fiz. 71, 1912-1915 (November 1976)

The explicit form of the electron density distribution $p_\infty(x)$ is calculated for a localized state in a one-dimensional disordered system. A general formula is obtained for the moments of $p_\infty(x)$.

PACS numbers: 71.20.+c, 71.50.+t

The question of the character of the electronic states in a one-dimensional disordered system was investigated by a number of workers (see the review by Mott^[1]). Mott and Twose^[2] have shown that all states in such a system are localized. The asymptotic form of the electron density for a localized state as $|x| \rightarrow \infty$ is essentially exponential. The argument of the exponential for certain models was determined by a number of workers.^[3-6] A more correct asymptotic expansion, which includes the pre-exponential factor, was obtained by Mel'nikov, Rashba, and the author^[7] with the aid of a method developed by Berezinskii.^[3] In the present paper the same method is used to obtain the explicit form of the distribution of the electron density of the localized state $p_\infty(x)$ for arbitrary x .

We consider a system of noninteracting electrons with a dispersion law $\varepsilon(p)$, situated in the field of randomly disposed centers $V(x)$. The random potential $V(x)$ is characterized by a correlator $U(x-x')$

$$U(x-x') = \langle V(x)V(x') \rangle. \quad (1)$$

The angle brackets denote here averaging over the realizations of the random potential. The electron scattering is considered in the Born approximation.

It was shown in the preceding paper^[7] that for this model the distribution of the electron density of the localized state $p_\infty(x)$, obtained from the expression for the long-time density correlator, is given by

$$p_\infty(x) = \frac{2}{\pi^2 l_i^-} \int_0^\infty \eta d\eta \operatorname{sh} \pi \eta \exp\left(-\frac{\eta^2+1}{4l_i^-} |x|\right) \times \int_0^\infty z dz K_1(z) K_{i\eta}(z) \int_0^\infty \xi d\xi K_1(\xi) K_{i\eta}(\xi), \quad (2)$$

where K_1 and $K_{i\eta}$ are Bessel functions, and l_i^- is the mean free path calculated from the Born amplitude of the impurity backscattering:

$$\frac{1}{l_i^-} = \frac{1}{v^2(\varepsilon)} \int_{-\infty}^\infty U(x) e^{2ip(\varepsilon)x} dx, \quad (3)$$

here $v(\varepsilon)$ is the velocity of an electron with energy ε , and $p(\varepsilon)$ is its momentum.

The integral with respect to z and ξ in (2) can be calculated exactly (see^[8], formula (6.576)):

$$\int_0^\infty z dz K_1(z) K_{i\eta}(z) \int_0^\infty \xi d\xi K_1(\xi) K_{i\eta}(\xi) = \frac{1}{2} \left[\int_0^\infty z dz K_1(z) K_{i\eta}(z) \right]^2 = \frac{1}{8} \left[\Gamma\left(\frac{3+i\eta}{2}\right) \Gamma\left(\frac{1+i\eta}{2}\right) \Gamma\left(\frac{3-i\eta}{2}\right) \Gamma\left(\frac{1-i\eta}{2}\right) \right]^2. \quad (4)$$

Using also the known identity for the Γ function (formula (8.332) from^[8]), we obtain

$$\Gamma\left(\frac{3+i\eta}{2}\right) \Gamma\left(\frac{1+i\eta}{2}\right) \Gamma\left(\frac{3-i\eta}{2}\right) \Gamma\left(\frac{1-i\eta}{2}\right) = \frac{\pi^2}{2} \frac{1+\eta^2}{1+\operatorname{ch} \pi \eta},$$

$$p_\infty(x) = \frac{\pi^2}{16l_i^-} \int_0^\infty \eta d\eta \operatorname{sh} \pi \eta \left(\frac{1+\eta^2}{1+\operatorname{ch} \pi \eta} \right)^2 \exp\left(-\frac{1+\eta^2}{4l_i^-} |x|\right). \quad (5)$$